

Bioflotation of apatite and quartz: Particle size effect on the rate constant

<http://dx.doi.org/10.1590/0370-44672014680239>

Antonio G. Merma

Research Assistant,
Pontifical Catholic University of Rio de Janeiro -
Chemical and Materials Engineering
Rio de Janeiro - Rio de Janeiro - Brazil
anguz21@hotmail.com

Maurício Leonardo Torem

Professor,
Pontifical Catholic University of Rio de Janeiro -
Chemical and Materials Engineering
Rio de Janeiro - Rio de Janeiro - Brazil
torem@puc-rio.br

Abstract

This work deals with the fundamental aspects of apatite and quartz bioflotation using *R. opacus* bacteria as a bioreagent. It was observed that the flotability of both minerals depends on the pH value and the mineral particle size. The maximum flotability of both minerals was presented at a pH value of 5, achieving values of 90% and 14% for apatite and quartz, respectively, after seven minutes of flotation. The kinetics analysis showed that the smaller the apatite particle size, the lower its bioflotation rate value. On the other hand, the smaller the quartz particle size, the higher its bioflotation rate value. The first-order kinetic model better fitted the experimental data of both minerals, and a logarithmic relationship between particle size and kinetic rate constant was observed.

keywords: bioflotation; bioreagents; particle size; rate constant; apatite; quartz.

1. Introduction

Currently, it is believed that mineral biobeneficiation is an emerging technology due principally its environmental and technological applications (Merma *et al.*, 2013). The most significant application is related to the depletion of the environmental impact, generated by the use of conventional flotation reagents (Sharma and Forssberg, 2001). Since its early years of research, the core of the study and development of mineral bioprocessing (bioflotation and biocoagulation) has been set on the proper understanding of its fundamental aspects. A standard fundamental bioflotation study is normally conducted with pure mineral samples and deals with microorganism growth, equilibrium adsorption fundamentals, flotation and/or flocculation studies; some of them are more specific and may embrace bacterial adsorption thermodynamics (Sharma and Forssberg, 2001; Botero *et al.*, 2008; Farahat *et al.*, 2008, 2009, 2010), kinetics of bioadsorption of the bioreagent onto the mineral surface

(Tan and Chen, 2012). Moreover, some works (Sharma and Forssberg, 2001; Sarvamangala *et al.*, 2011, 2012, 21013; Pakudone and Natarajan, 2011) deal with the use of microorganism by-products, extracellular polymeric substances (EPS), or the so-called biosurfactants produced by the microorganisms (Natarajan, 2006). Additionally, literature depicts some relevant works on the bioflotation of ores (Mehrabani *et al.*, 2010; Khoshdast *et al.*, 2012; Elmahdy *et al.*, 2013) and of coal (Abdel-khalek and El-midany, 2013; El-midany and Abdel-Khalek, 2014). The aim of these works was to evaluate the performance of these eco-friendly reagents as biocollectors, biodepressors or biofrothers.

Although Bioflotation and flotation processes are governed by the same fundamental physicochemical principles, very little is known about the influence of the physical properties of minerals on bioflotation. As example, it is known that there is an optimum particle size range for a given

flotation system (Santana *et al.*, 2008), but will this range also optimize bioflotation?

Moreover, before the bioprocessing of a determined ore could be considered suitable, it is necessary to know the response of each mineral species, present in the ore, to bioflotation. Brazilian igneous phosphate ores are associated with several gangue minerals, such as quartz, magnetite, carbonates and silicates (Oliveira, 2005). Thus, in order to establish the application of a microorganism in the bioflotation of phosphate ores, a detailed bioflotation study of each component is necessary, principally for apatite, quartz, silicate, calcite, and probably dolomite.

Considering the before mentioned situation, the aim of this study was to investigate the effect of particle size on mineral bioflotation. Apatite and quartz samples are the minerals under study and *Rhodococcus opacus* the strain to act as biocollector and biofrother. Moreover, a kinetic analysis of the flotability is used to help the understanding of the process.

2. Materials and methods

2.1 Sample preparation

The fluorapatite sample, $\text{Ca}_5[\text{PO}_4]_3(\text{Cl}, \text{F}, \text{OH})$ (42.33% P_2O_5

and 54.39% CaO), and the pure quartz sample were provided by a local

supplier (Estrada Mining, Belo Horizonte, Minas Gerais). The samples

were crushed and then dry-screened to -3 mm, followed by dry-grinding in a porcelain mortar and then wet-screened to the desired size fractions. Then, the quartz sample was rested

in a KOH (0.1 M) solution during 24 hours to remove the impurities present onto the quartz surface. Afterwards, the samples were washed several times with double-distilled water until the

pH suspension achieved the initial pH. Finally, the samples were dried at room temperature and stored in a desiccator, until their use in the various tests.

2.2 Microorganisms, Culture and growth

According to Mesquita *et al.* (2003) the non-pathogenic *Rhodococcus opacus* strain presents a hydrophobic behavior (Contact angle around 70°), and it was the main reason for its use in this study. The strain, supplied by the Brazilian Collection of Environmental and Industrial Microorganisms (CBMAI-UNICAMP), was developed in a YMG solid media, containing: glucose 10.0 g L⁻¹, peptone 5.0 g L⁻¹, malt extract 3.0 g L⁻¹, yeast extract 3.0 g L⁻¹, and agar-agar 12 g L⁻¹.

Stocks of the bacteria were prepared and renewed frequently using this medium in Petri plates and storing them in a freezer at 15 °C. Next, the cells were sub-cultured in a YMG liquid medium, containing: glucose 10.0 g L⁻¹, peptone 5.0 g L⁻¹, malt extract 3.0 g L⁻¹ and yeast extract 3.0 g L⁻¹) at pH 7.2, on a rotary shaker at 175 rpm and 28 °C, during 72 h. Time needed for the bacterial cells to reach the beginning of the stationary phase of their growth. After that, the cellular suspension was

centrifuged at 3500 rpm during 10 min, followed by twice re-suspensions with deionized water, in order to remove any culture remainder; and then the cells were re-suspended in a 10⁻³ M NaCl solution. Finally, the cellular concentrate was inactivated in an autoclave to avoid further bacterial development. The concentration of the biomass was measured by using a spectrophotometer (UV-1800, Shimadzu UV-spectrophotometer) at a wavelength of 620 nm.

2.3 Flotation experiments

The microflotation study was conducted in a modified *Hallimond* tube. The mineral sample (1.0 g) was placed in the tube (volume: 0.16 L) containing a cellular suspension of known concentration. The suspension was mixed by constant stirring for about 5 minutes

(conditioning time), and then the pH was adjusted to the desired value with diluted HCl and NaOH solutions. Finally, the mineral flotation tests were carried out using an air flow of 15 ml min⁻¹ during a known time of minutes. The floated and non-floated fractions

were carefully separated, washed, dried and weighed in order to calculate the flotability. For the kinetics analyzes, the flotation was conducted during 7 min. and samples were collected after 0.50, 0.75, 1.00, 2.00, 3.00, 5.00 and 7 minutes of flotation.

2.4 Kinetics of bioflotation

The flotation rate can be defined as a measure of the flotation recovery expressed per unit of time (Bulatovic, 2007), it means, the amount of floated particles with regard to flotation time (Hernández and Calero, 2001). Different models have been proposed to evaluate the flotation kinetic behavior (Hernández and Calero, 2001; Hernández *et al.*, 2005; Yalcin and Kelebek, 2011; Polat and Chander, 2000; Su *et al.*, 1998; Zhang *et al.*, 2013).

Although there are many approaches to describe mineral flotation kinetics, the most widely used models are based on analogy with a chemical reactor, which means that a flotation cell can be approximated by perfectly mixed CSTR (Hernández *et al.*, 2005; Yalcin and Kelebek, 2011; Polat and Chander, 2000; Su *et al.*, 1998; Zhang *et al.*, 2013). Considering, that bioflotation and flotation are governed for the same physicochemical

principles, it is correct to assume that previous kinetic models can be used to describe the kinetics of bioflotation. This was also assumed in some bioflotation works (Amini *et al.*, 2009; Pecina *et al.*, 2009; Mehrabani *et al.*, 2010; Khoshdast *et al.*, 2012). Therefore, this paper also presents a kinetic analysis of the mineral bioflotation using kinetic models based on chemical reactor analogy. This equation may be expressed by:

$$\frac{dC}{dt} = -k \cdot C^n \quad (1)$$

$$R(\%) = \left(1 - \frac{C}{C_0}\right) \times 100 \quad (2)$$

where “C” is the concentration of solids, “C₀” is the initial concentration, “t” flotation time, “n” order of the process, and “k” is the flotation rate constant. Considering that the mineral recovery (R) is a function of C (equation 2), we can obtain the models in function of such recovery.

It is commonly accepted that the order “n” and the rate constant “k” are

dependent on the flotation conditions, some related to ore characteristics such as mineralogy, particle size and surface chemistry, and others, related to operations conditions such as air flow rate, reagents, etc. (Pecina *et al.*, 2009; Deo *et al.*, 2001; Yalcin and Kelebek, 2011). According to Brozek and Mlynarczykowska (2007), the flotation kinetics order changes during the process summarized

as follows: at the beginning, the particles with the uppermost flotation properties may present a zero order value, but with time, the particles present a decreasing ability to float and, simultaneously, the order of the flotation kinetics increases. In this work, however, three approaches to determine the rate constant were considered, explicitly: first-order (n=1), second-order (n=2) and non-integral-

order models. The integrated equations

for the three models mentioned are shown in Table 1.

| Model | Formula | Description |
|-----------------------------------|---|---|
| Classical first order model (n=1) | $\ln(1-R) = K_1 \cdot t$ | R = recovery percentage of the mineral. |
| Second order (n=2) | $\frac{R}{(1-R)} = k_2 \cdot m_0 \cdot t$ | m_0 = Initial mass of the mineral in the flotation cell. |
| Non-integral order | $\ln\left(\frac{1}{1-\frac{R}{R^\infty}}\right) = k_{ni} \cdot t$ | R^∞ = recovery percentage of the mineral at infinite time. |

Table 1
Description of the three flotation kinetic models used in this paper

3. Results and discussion

3.1 Flotation studies

The microflotation studies were carried out in order to evaluate the effect of the mineral particle size and pH on the bioflotation of apatite and quartz, using

the *R. opacus* bacteria as biocollector. It was shown that the *R. opacus* strain has a strong capability of acting either as a biocollector or a biofrother (Merma *et*

al., 2013). This previous work pointed out that the highest flotability value of both minerals was achieved using 0.15 g L^{-1} of the bacteria.

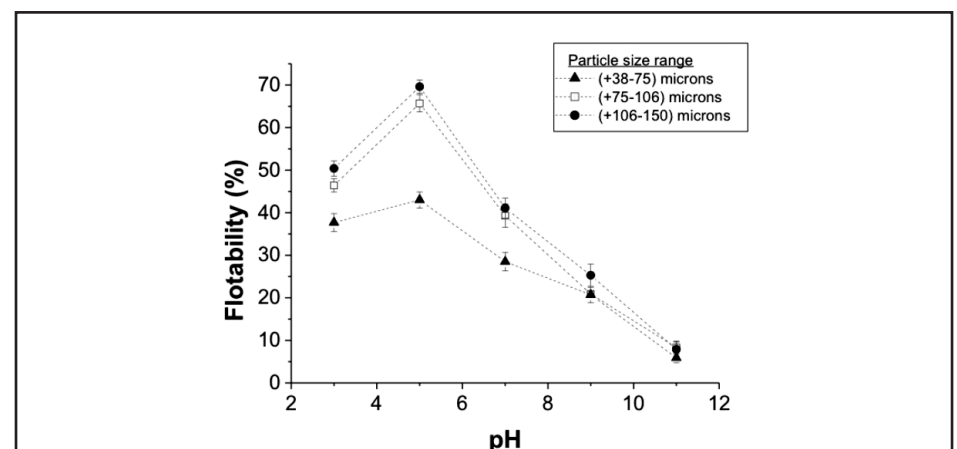
3.1.1 Effect of the pH and particle size on the bioflotation of quartz and apatite

The pH of the solution is one of the most important factors affecting the bioflotation. This affects the speciation onto the mineral surface as well as the activation of the functional groups present on the wall cell. Thus, the pH value affects the surface properties of the mineral, as the hydrophobicity and, therefore, the bioflotation response of the minerals. The flotability of apatite and quartz as a function of pH value is presented in Figs. 1 and 2, respectively. It can be observed that for both minerals, the highest flotability was presented in an acidic medium, around pH 5, after two minutes of flotation. Moreover, in a very acidic medium, the flotability presented lower values, whereas declines were observed in an alkaline medium. This is in accordance with several bioprocessing studies (Farahat *et al.*, 2008, 2010, 2012; Mesquita *et al.*, 2003; El-midany and Abdel-Khalek, 2014), where the highest flotability of the minerals was achieved at

around the isoelectric point value of the bacteria, which generally has an acidic pH value. At this point, it is believed that the electrostatic repulsion between mineral particles and bacterial cells is suppressed, and specific interactions would let the adsorption of the bacterial cells onto the mineral surface, which would increase the hydrophobicity of the mineral and hence a higher flotability would be observed. It was also observed that particle size affected in a different form the flotability of quartz and apatite. The smaller the particle size, the higher the quartz flotability value, achieving flotability values around 18% and 10% for the finest and the coarsest particle size, respectively (Fig.2); while for apatite the smaller the particle size the lower the flotability value, achieving flotability values around 69% and 43% for the coarsest and the finest particle size, respectively (Fig. 1). The behavior of the quartz sample can be explained due to the fact that microorganism cells essen-

tially did not adsorb onto the surface of the quartz particles, which consequently maintain hydrophilic. Hence the recovery of the quartz particles depends on the air flow (entrainment). Therefore, small quartz particles, with lower mass, could be more easily carried into the concentrate by mechanical entrainment (Konopacka and Drzymala, 2010). On the other hand, the hydrophobized apatite particles presented an opposite behavior. It is possible to mention two factors which would explain the lower flotability value of apatite attained when the smallest particle size was used: (1) there was higher collector consumption due to the larger surface area of the smaller particles (Smith, 1997) and (2) the small particles present a lower efficiency in the bubble-particle collision (Chen jin *et al.*, 1998). According to the previous, a lower flotability of the apatite would be expected when the finest size range was used, only if the initial bacterial concentration was maintained.

Figure 1
Bioflotation of apatite as a function of pH at different particle sizes; bacterial concentration 0.15 g L^{-1} , time of flotation: 2min.



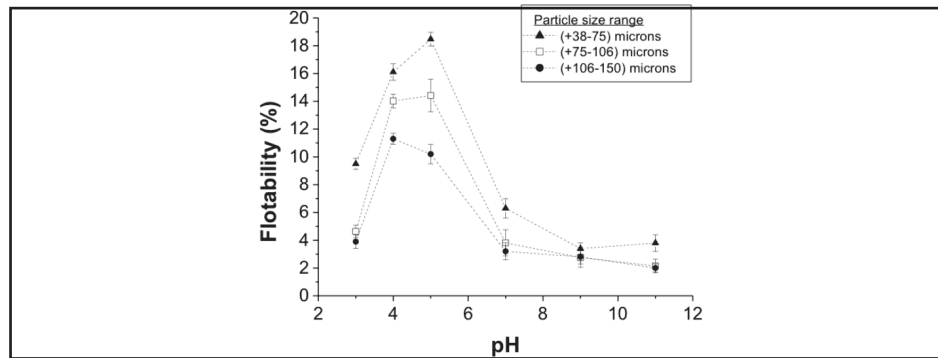


Figure 2
Bioflotation of quartz as a function of pH at different particle sizes; bacterial concentration 0.15 g L⁻¹. Flotation of Time: 2 min.

3.1.2 Effect of the flotation time on the bioflotation of quartz and apatite

The flotability of apatite and quartz as a function of time for different particle sizes can be seen in Fig. 3 and Fig. 4, respectively. It shows that the flotability of apatite increased regularly as a function of time, but decreased as the particle size was increased. Achieving flotability values around 92% and 80% for the coarsest and the finest particle sizes. On the other hand, quartz presented low values of flotability (around 14%)

for the coarsest size range, increasing monotonically as a function of time. Furthermore, for finer particles: the higher the flotation time, the higher its flotability values, achieving around 52% after seven minutes of flotation.

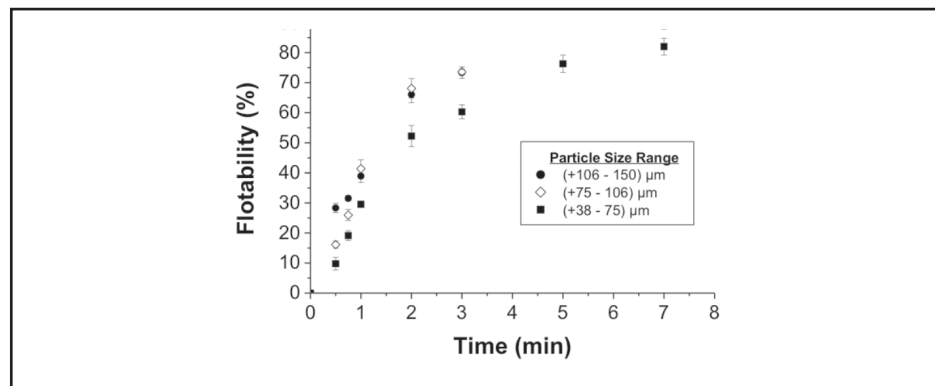


Figure 3
Bioflotation of apatite as a function of time at different particle sizes; pH: 5; bacterial concentration 0.15 g L⁻¹.

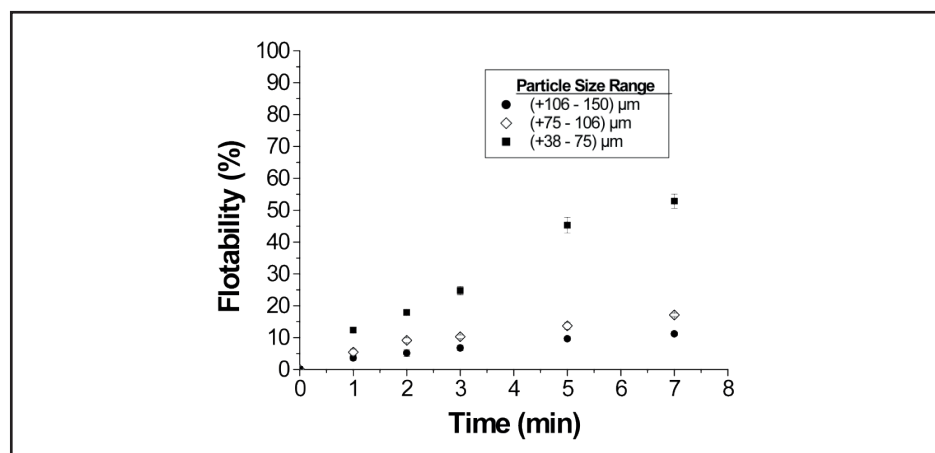


Figure 4
Bioflotation of quartz as a function of time at different particle sizes; pH: 5; bacterial concentration 0.15 g L⁻¹.

3.2 Kinetics studies

The kinetic study was developed in order to have a better understanding of the effect of particle size on the bioflotation rate of apatite and quartz. As mentioned before, the existing literature

shows few works dealing with bioflotation kinetics, hence, this subject is not very well known. However, as in flotation, bioflotation should be controlled by surface characteristics and knowing that

the flotation recovery depends on the particle size fraction, (Santana *et al.*, 2008; King, 1982) as well as the rate constant (Jameson, 2012), it should be right to affirm the same about bioflotation.

3.2.1 Apatite

The flotability of apatite (plotted in Fig. 3) has been examined from a kinetics point of view, using the three approaches mentioned before, in order to determine the rate constant. The

kinetics parameters obtained from this analysis are given in Table 2, with their corresponding correlation coefficients (r^2) obtained from a linear regression. From these coefficients, it was able to

assume that the first-order model best fitted the experimental data. This supposingly is correct, since, the mineral suspension inside the *Hallimond* tube was perfectly mixed by magnetic stir-

ring. Moreover, the second-order model also fitted the results; however, this effect was attributed to the small amount of particles inside the *Hallimond* tube (1 g), as pointed out by several authors (Bulatovic, 2007; Yalcin and Kelebek, 2011; Nguyen and Schulze, 2004; Hernáinz

and Calero, 1996). Additionally, it was observed that the non-integral model also adjusted the experimental data. According to several authors (Hernáinz and Calero, 2001; Hernáinz *et al.*, 2005; Zhang *et al.*, 2013), there exists a direct relationship between the flotation rate

constant and the particle size. From the Table 2, it was possible to observe that the rate constant decreased as the particle size decreased, but, this effect was not observed for the non-integral model. Consequently, this model was rejected in spite of its good correlation.

Table 2
Kinetics parameters
obtained from three different kinetics
models in the bioflotation of apatite

| Particle Size (μm) | Apatite | | | | | |
|------------------------------------|-----------------------------|-------|---|-------|---------------------------|-------|
| | 1 ^o order | | 2 ^o order | | Non-integral order | |
| | k_1 (min^{-1}) | r^2 | k_2 (g min^{-1}) ⁻¹ | r^2 | k (min^{-1}) | r^2 |
| +106 -150 | 0.449 | 0.95 | 2.094 | 0.88 | 0.841 | 0.858 |
| +75 -106 | 0.392 | 0.924 | 1.375 | 0.932 | 0.8721 | 0.904 |
| +38 -75 | 0.271 | 0.967 | 0.624 | 0.983 | 0.503 | 0.984 |

According to the authors, the re-

(3)

where, the exponent “m” could be calculated from the logarithmic representation of “ k_q ” against the average particle size “d”.

Thus, the logarithmic representation of “ k_q ” against the average particle size can be seen in Fig. 5. The linear regression showed that the first-order and second-order models attained high

relationship between rate constant and

particle size is of the kind:

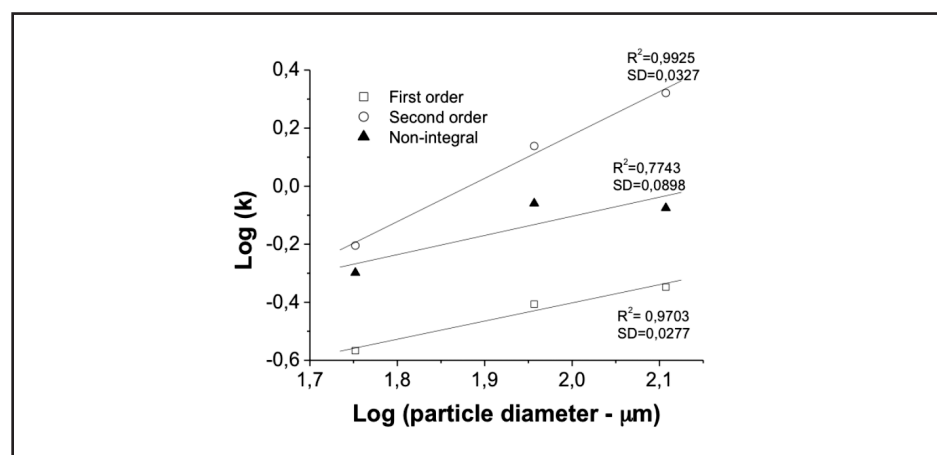
$$k_q \propto d^m$$

correlation coefficient values, and therefore, verifies the previously mentioned relationship. On the other hand, the low correlation value attributed to the non-integral model did not support a relationship between particle size and rate constant.

Therefore, considering the previous analysis, it was confirmed that

the apatite bioflotation experimental data were properly fitted by using the first-order kinetic model. And the rate constant for apatite bioflotation decreased as the particle size decreased. These results are in good accordance to those observed by Su *et al.* (1998) and by Abkhoshk *et al.* (2010) for apatite and coal flotation, respectively.

Figure 5
Logarithmic representation
of “k” in function of particle size,
applied to three different kinetics
models in the bioflotation of apatite.



3.2.2 Quartz

Similarly, the kinetics parameters obtained for the bioflotation of quartz are given in Table 3, with their corresponding correlation coefficients (r^2) obtained from the linear regression. From the results, it is possible to observe a similar behavior than that observed in the kinetics bioflota-

tion of apatite. It means that the first-order model best fitted the experimental data, in spite of the good adjusted presented for the non-integral model. Model discarded because according to the Fig. 6 it was not observed a clear relation between the rate constant and the particle size and due to

its lesser correlation coefficient.

Therefore, considering the previous analysis, it was confirmed that the quartz bioflotation experimental data were properly fitted by using the first-order kinetic model. The results clearly showed that the rate constant for quartz bioflotation,

k, increased as the particle size decreased. This behavior is in good accordance with those observed by Yalcin and Kebelec (2011) and by Yekeler and Sonmez (1997) in the flotation of a pyritic gold ore and

talc, respectively.

From this study, it is clear that the *Rhodococcus opacus* bacteria can be used as a biocollector and as biofrother during the flotation of apatite, even in

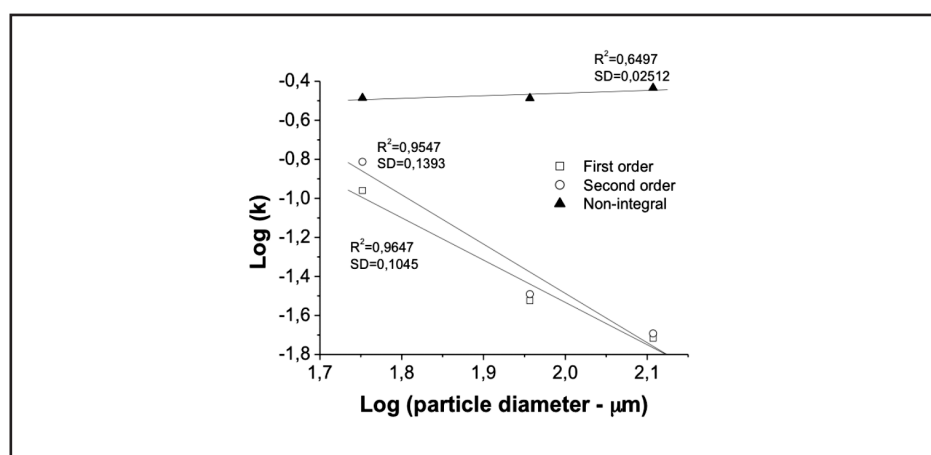
fine particle sizes and in an acidic pH range (between values around 3 and 5). Moreover, the bioflotation of apatite can be represented by using the first-order kinetic model.

Quartz

| Particle Size (µm) | 1 ^o order | | 2 ^o order | | Non-integral order | |
|--------------------|----------------------------|----------------|-----------------------------|----------------|--------------------------|----------------|
| | k_1 (min ⁻¹) | r ² | k_2 (g min) ⁻¹ | r ² | k (min ⁻¹) | r ² |
| | +106 -150 | 0.0192 | 0.90 | 0.0203 | 0.91 | 0.368 |
| +75 -106 | 0.0299 | 0.90 | 0.0323 | 0.90 | 0.326 | 0.986 |
| +38 -75 | 0.1097 | 0.98 | 0.1539 | 0.97 | 0.327 | 0.878 |

Table 3 Kinetics parameters obtained from three different kinetics models in the bioflotation of quartz

Figure 6 Logarithmic representation of “k” in function of particle size, applied to three different kinetics models in the bioflotation of quartz.



4. Conclusions

The bioflotation of apatite and quartz particles using *R. opacus* as bio-reagent was found to be dependent on the pH and the mineral particle size. The highest flotability value of both minerals was achieved at pH 5. For the coarsest fractions, the apatite presented its higher flotability value (around 70%) after 2 min. of flotation, while the quartz presented its higher flotability value (around

18%) for the finest particle size. The results showed that the bioflotation rate of apatite is higher, achieving flotability values of around 92% and 52% for apatite and quartz, respectively, after 7 minutes of flotation. Also, it was observed that the bioflotation rate of the apatite decreased as the particles sizes decreased, in contrast to the bioflotation rate of quartz, which increased. Finally, the first-order

kinetic model showed a better fit to the experimental data of both minerals and a direct relationship between the rate constant and the mineral particle size was observed. Nevertheless, the non-integral models also fitted the experimental data. However, it was not possible to observe a clear relationship between the rate constant and particle size when this model was used.

5. References

ABKHOSHK, E., KOR, M., REZAI, B. A study on the effect of particle size on coal flotation kinetics using fuzzy logic. *Expert Systems with applications*. v. 37, p. 5201-5207, 2010.

ABDEL-KHALEK, M.A., EL-MIDANY, A.A. Adsorption of *Paenibacillus polymyxa* and its impact on coal cleaning. *Fuel Processing Technology*. v. 113, p. 52-56, 2013.

AMINI, E., OLIAZADEH, M., KOLAHDOOZAN, M. Kinetic comparison of biological and conventional flotation of coal. *Minerals Engineering*. v. 22, p. 344-347, 2009.

BOTERO, A.E.C., Torem, M.L., Mesquita, L.M.S. Surface chemistry fun-

- damentals of biosorption of *Rhodococcus opacus* and its effect in calcite and magnesite flotation. *Minerals Engineering*, v. 21, n. 1, p. 83-92, 2008.
- BROZEK, M., Mlynarczykowska, A. Analysis of Kinetics models of batch flotation. *Physicochemical Problems of Mineral Processing*, v. 41, p. 51-65, 2007.
- BULATOVIC, S.M. Theoretical Aspects of Flotation. In: *Handbook of flotation Reagents. Chemistry, theory and practice: Flotation of sulfides ores*. Elsevier, 2007. (Chapter 6: Summary).
- CHEN, JIN, CHEN, DAGAO, CHEN, TINZHONG. Technological innovation and theoretical approach to shear washing for a refractory manganese ore. Production and Processing of fine particles. Plumpton (ed.). Canadian Institute of Mining and Metallurgy, p. 427-438, 1998.
- DEO, N., NATARAJAN, K.A., Somasundaran, P. Mechanisms of adhesion of *Paenibacillus polymyxa* onto hematite, corundum and quartz. *International Journal of Mineral Processing*, v. 62, p. 27-39, 2001.
- ELMAHDY, A.M., EL-MOFTY, S.E., ABDEL-KHALEK, M.A., ABDEL-KHALEK, N.A., El-Midany, A.A. Bacterially induced phosphate-dolomite separation using amphoteric collector. *Separation and Purification Technology*, v. 102, p. 94-102, 2013.
- EL-MIDANY, A.A. ABDEL-KHALEK, M.A. Reducing sulfur and ash from coal using *Bacillus subtilis* and *Paenibacillus polymyxa*. *Fuel*, v. 115, p. 589-595, 2014.
- FARAHAT, M., HIRAJIMA, T., SASAKI, K. DOI, K., Adhesion of *Escherichia coli* onto quartz, hematite and corundum: Extended DLVO theory and flotation behavior. *Colloids and surfaces B: Biointerfaces*, v. 74, p. 140-149, 2009.
- FARAHAT, M., HIRAJIMA, T., SASAKI, K. Adhesion of *Ferroplasma acidiphilum* onto pyrite calculated from the extended DLVO theory using the van Oss-Good-Chaudhury approach. *Journal of colloids and interface science*, v. 29, p. 594-601, 2010.
- FARAHAT, M., HIRAJIMA, T., SASAKI, K., AIBA, Y., DOI, K. Adsorption of *SIP E. coli* onto quartz and its applications in froth flotation. *Minerals Engineering*, v. 21, 389-395, 2008.
- HERNÁINZ, F., CALERO, M. Flotation rate of celestite and calcite. *Chemical Engineering Science*, v. 51, n. 1, p. 119-125, 1996.
- HERNÁINZ, F., CALERO, M. Froth flotation: kinetic models based on chemical analogy. *Chemical Engineering and Processing*, v. 40, p. 269-275, 2001.
- HERNÁINZ, F., CALERO, M., BLÁZQUEZ, G. Kinetic considerations in the flotation of phosphate ore. *Advanced Powder Technology*, v. 16, n. 4, p. 347-361, 2005.
- JAMESON, GRAEME, J. The effect of surface liberation and particle size on flotation rate constants. *Minerals Engineering*, v. 36-38, p. 132-137, 2012.
- KHOSHDAST, H., SAM, A., MANAFI, Z. The use of rhamnolipid biosurfactants as a frothing agent and a sample copper ore response. *Minerals Engineering*, v. 26, p. 41-49, 2012.
- KING, R.P. Principles of flotation, chapter 11. South African institute of Mining and Metallurgy Monograph series. Johannesburg, 1982.
- KONOPACKA, Z., DRZYMALA, J. Types of particles recovery—water recovery entrainment plots useful in flotation research. *Adsorption*, v. 16, p. 313-320, 2010.
- MEHRABANI, J.V., NOAPARAST, M., MOUSAVI, S.M., DEHGHAN, R., RASSOLI, E., HAJIZADEH, H. Depression of pyrite in the flotation of high pyrite low-grade lead-zinc ore using *Acidithiobacillus ferrooxidans*. *Minerals Engineering*, v. 23, n. 1, p. 10-16, 2010.
- MERMA, A.G., TOREM, M.L., MORAN, J.V., MONTE, M.B.M. On the fundamental aspects of apatite and quartz flotation using a gran positive strain as a bioreagent. *Minerals Engineering*, v. 48, p. 61-67, 2013.
- MESQUITA, L.M.S., LINS, F.A.F., TOREM, M.L. Interaction of a hydrophobic bacterium strain in a hematite-quartz flotation system. *International Journal of Mineral Processing*, v. 71, p. 31-44, 2003.

- NATARAJAN, K.A., Microbially-induced mineral flotation and flocculation: prospects and challenges. In: INTERNATIONAL MINERAL PROCESSING CONGRESS, 23. Proceedings... p. 487-498, 2006.
- NGUYEN, A.V., SCHULZE, H.J., Colloid science of flotation. In: *Surfactant Series*. New York: Marcel Dekker, Inc., 2004. v. 118. (Chapter 30).
- OLIVEIRA, J.A. *Saponification degree of vegetable oils at selective flotation of apatite from carbonates ore*. Ouro Preto: Department of Mining Engineering - UFOP, 2005. (MSc. Dissertation in Portuguese).
- PAKUDONE, S.U., NATARAJAN, K.A. Microbially induced separation of quartz from calcite using *Saccharomyces cerevisiae*. *Colloids and surfaces B: Biointerfaces*, v. 88, p. 45-50, 2011.
- PECINA, E.T., RODRIGUEZ, M., CASTILLO, P., DIAZ, V. ORRANTIA, E. Effect of *Leptospirillum ferrooxidans* on the flotation kinetics of sulphide ores. *Minerals Engineering*, v. 22, p. 462-468, 2009.
- POLAT, M., CHANDER, S. First-order flotation kinetics models and methods for estimation of the true distribution of flotation rate constants. *International Journal of Mineral Processing*, v. 58, p. 145-166, 2000.
- SANTANA, R.C., FARNESE, A.C.C., Fortes, M.C.B., Ataíde, C.H, Barrozo, M.A.S. Influence of particle size and reagent dosage on the performance of apatite flotation. *Separation and Purification Technology*, v. 64, p. 8-15, 2008.
- SARVAMANGALA, H., NATARAJAN, K.A. Microbially induced flotation of alumina, silica/calcite from haematite. *International Journal of Mineral Processing*, v. 99, p. 70-77, 2011.
- SARVAMANGALA, H., NATARAJAN, K.A., GIRISHA, S.T. Microbially-induced pyrite removal from galena using *Bacillus subtilis*. *International journal of Mineral Processing*, v. 120, p. 15-21, 2013.
- SARVAMANGALA, H., NATARAJAN, K.A., GIRISHA, S.T. Biobeneficiation of Iron ores. *International Journal of Mining Engineering and Mineral Processing*. v. 1, n. 2, p. 21-30, 2012.
- SHARMA, P.K., RAO, K.H., FORSSBERG, K.S.E., NATARAJAN, K.A., Surface chemical characterization of *Paenibacillus polymyxa* before and after adaptation to sulfide minerals. *International Journal of Mineral Processing*. v. 63, p. 3-25, 2001.
- SMITH, R.W. Bacteria as flotation reagents for the flotation of a dolomitic phosphate rock. Florida Institute of Phosphate Research (FITR) – University of Nevada Reno. n. 02, p. 106-131, January 1997.
- SU, FENWEI, RAO, K.H., FORSSBERG, K.S.E., Samskog, P.O. The influence of temperature on the kinetics of apatite flotation from magnetite fines. *International Journal of Mineral Processing*. v. 54, p. 131-145, 1998.
- TAN, S.N., CHEN, M. Early stage adsorption behavior of *Acidithiobacillus ferrooxidans* on minerals I: an experimental approach. *Hydrometallurgy*, v. 119-120, p. 87-94, 2012.
- YALCIN E., KELEBEK, S. Flotation Kinetics of a pyritic gold ore. *International Journal of Mineral Processing*, v. 98, p. 48-54, 2011.
- YEKELER, M., SONMEZ, I. Effect of the hydrophobic fraction and particle size in the collectorless column flotation kinetics. *Colloids and surfaces A: Physicochemical and Engineering Aspects*, v. 121, p. 9-13, 1997.
- ZHANG, H., LIU, J., CAO, Y., WANG, Y. Effects of particle size on lignite reverse flotation kinetics in the presence of sodium chloride. *Powder Technology*, v. 246, p. 658-663, 2013.

Received: 12 December 2014 - Accepted: 11 June 2015.